Cost-Effective Strategies for Infectious Diseases: A Multi-Objective Framework with Interactive Dashboard

Jongmin Lee[1], Renier Mendoza[2,3], Victoria May P. Mendoza[2,3], Eunok Jung[1*]

[1]Department of Mathematics, Konkuk University, Seoul, 05029, Korea.
[2]Institute of Mathematics, University of the Philippines Diliman, Quezon City, 1101, Philippines.
[3]Computational Science Research Center, College of Science, University of the Philippines Diliman, Quezon City, 1101, Philippines.

*Corresponding author(s). E-mail(s): junge@konkuk.ac.kr;
Contributing authors: ljm1729@konkuk.ac.kr;
rmendoza@math.upd.edu.ph; vmpaguio@math.upd.edu.ph;

Abstract

During an infectious disease outbreak, policymakers must balance medical costs with social and economic burdens, seeking interventions that minimize both. To support this decision-making process, we developed a framework that integrates multi-objective optimization, cost–benefit analysis, and an interactive dashboard. This platform enables users to input cost parameters and immediately obtain a cost-optimal intervention strategy. As an example, we applied the framework to the early outbreak of COVID-19 in Korea. The results show that cost-optimal solutions for costs per infection ranging from 2,978 USD to 170K USD exhibited similar patterns. This highlights that once the cost per infection is specified, our approach generates the corresponding cost-optimal solution without additional calculations. Our framework supports decision-making by accounting for the trade-off between policy and infection costs. It delivers rapid optimization and cost–benefit analysis results, enabling timely and informed decision-making during critical phases of a pandemic.

Keywords: Infectious disease, Mathematical modeling, Multi-objective optimization, Cost-benefit analysis, Dashboard

Introduction

During the COVID-19 pandemic, governments faced a trade-off problem between minimizing infections and the economic burden from non-pharmaceutical interventions, such as lockdowns and gathering restrictions [1]. Identifying an optimal strategy is challenging since multiple possible strategies may satisfy Pareto optimality according to health and economic costs [2–5]. Decision-makers face two central questions: (1) What is the best intervention strategy to minimize the costs of interventions and infections simultaneously? and (2) What are the reasonable costs of these interventions and infections? In this research, we answer these questions based on a research framework with an COVID-19 example.

In recent decades, increasing air travel and the growing concentration of populations in urban areas have accelerated the global spread of infectious diseases such as SARS, H1N1 influenza, MERS, and COVID-19 [6, 7]. Although traditional measures such as isolation, quarantine, and community containment were successfully implemented during the 2003 SARS outbreak [8], most countries were unable to control the spread of COVID-19 in 2020 using these standard measures [9]. These contrasting outcomes highlight the urgent need for more acceptable and cost-effective intervention strategies, particularly for emerging respiratory infectious diseases for which pharmaceutical interventions may not be immediately available [10].

Researchers have studied mathematical modeling, parameter estimation, optimization, and cost-benefit analysis for infectious diseases. Compartmental models [11, 12], stochastic models [13–15], agent-based models [16–19], and network models [20–22] are employed to capture the transmission dynamics of infectious diseases

and the interactions among individuals. Based on these modeling methods, optimization can identify the most effective non-pharmaceutical or pharmaceutical intervention strategy [23]. Optimal control theory has been utilized to determine time-varying non-pharmaceutical interventions (NPIs) that minimize a single objective, typically either disease burden or economic loss [24–27]. To minimize both infection and intervention costs simultaneously, multi-objective optimization is adopted, identifying Pareto-optimal strategies [28–32]. Note that single-objective optimization requires predefined weights or costs prior to the optimization process, whereas multi-objective optimization does not require such preset parameters in advance, thereby avoiding the need for extensive computational simulations repeatedly.

Since modeling and optimization results are theoretical, they need to be evaluated against actual costs and presented to users in a more accessible format. Cost-benefit analysis quantifies the efficiency of modeling or optimization results in various interventions during an epidemic of the disease. Paltiel et al. demonstrated that weekly testing is cost-effective under moderate transmission scenarios by comparing incremental cost-effectiveness ratios (ICER) to societal willingness-to-pay thresholds [33, 34]. Sandmann et al. evaluated the optimal timing of lockdowns that allowed for GDP losses of 2% to 15% per day [35], while Kohli et al. calculated ICER for vaccination campaigns in terms of averted infections and quality-adjusted life years [36]. To bridge the gap between complex modeling and policy practice, recent work has proposed multi-objective results. For example, a study presents a web tool to explore trade-offs in influenza control, but few platforms allow real-time adjustments of both epidemiological and economic parameters for emerging pathogens [37, 38]. Although many studies have analyzed infectious disease epidemics using the individual techniques mentioned, we developed a novel framework that synthesizes all of these methods into a single workflow. Research that simultaneously addresses both multi-objective optimization and cost-benefit analysis remains rare. Moreover, there is no

previous study that has translated such results into an intuitive dashboard that non-specialists in mathematical modeling can immediately use. Our work, therefore, offers a new approach that swiftly delivers modeling, optimization, and economic evaluation insights to decision-makers in a familiar format during the urgent situation of an epidemic or pandemic.

In this paper, we first introduce the research framework for general infectious diseases. Next, we present an application to the early phase of COVID-19 in Korea, which encompasses mathematical modeling, parameter estimation, multi-objective optimization, cost-benefit analysis, and the development of an interactive dashboard. Our contributions in this research are threefold. First, we propose a novel methodological approach that applies multi-objective optimization to address the inherent trade-offs in policy interventions, a strategy that can be generalized to other infectious diseases beyond COVID-19. Second, we reveal that there are only a few cost-optimal patterns of transmission reduction non-pharmaceutical intervention (NPI) strategies according to the infection cost. Third, the interactive dashboard offers an intuitive decision-support tool that streamlines the process of selecting and adapting optimal intervention policies, emphasizing the benefits of multi-objective optimization.

Results

To support decision-making in the early phase of infectious disease outbreaks, we developed a systematic research framework composed of five sequential processes, as illustrated by the orange diamonds in Figure 1. The framework begins with mathematical modeling, where an appropriate infectious disease model is formulated to reflect the characteristics of the outbreak. This model defines the disease compartments (e.g., susceptible, infected, recovered) and key parameters based on country-specific contexts and anticipated public health interventions. Next, parameter estimation is conducted to calibrate unknown parameters of the model using observed epidemiological data,

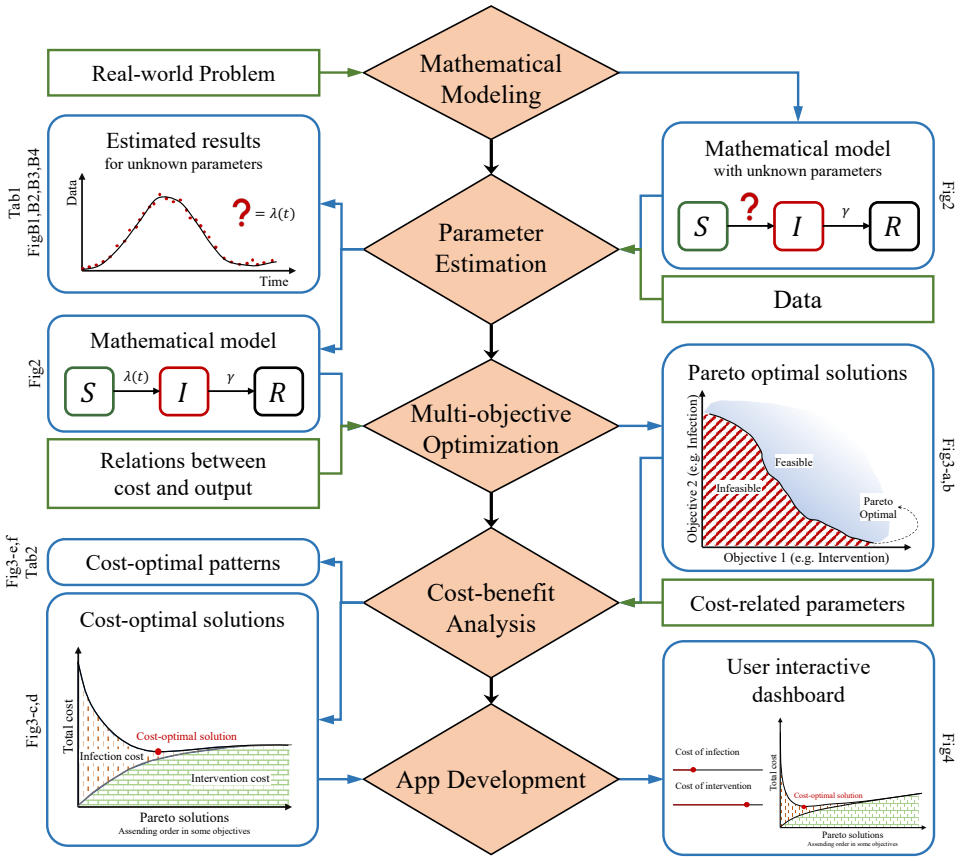

Fig. 1 Research framework for infectious diseases. Orange diamonds denote five steps of the framework, green rectangles represent required inputs, blue rounded rectangles summarize outputs with corresponding figures or tables.

such as case counts or hospitalization numbers. To enhance the robustness of this step, we performed sensitivity analysis and estimated the posterior distributions of parameters using Bayesian inference, which allows the model to closely reproduce the actual epidemic or outbreak dynamics.

In the third step, multi-objective optimization is applied to identify Pareto-optimal intervention strategies that balance competing objectives—minimizing both the cost of infection and the cost of intervention. These trade-offs are quantified by defining objective functions that rely on the relationship between model outputs (e.g., the

number of infections) and practical cost metrics. Notably, changes in the relationship between cost and output lead to different sets of Pareto-optimal and cost-optimal solutions, as demonstrated in Appendix **??**. Following this, cost-benefit analysis is employed to determine the most cost-effective intervention strategies based on pre-defined cost-related parameters. These parameters include, for example, the value of a statistical life, GDP loss due to lockdowns, quarantine costs, and fatality rates. These factors directly influence the selection of optimal strategies and can be adapted to reflect economic and societal differences across regions. Finally, we developed a web-based interactive dashboard to enable end-users—such as policymakers and public health officials—to explore and select intervention strategies based on their own cost assumptions and constraints. The dashboard provides real-time visualization of cost-optimal outcomes under various parameter settings, thereby offering actionable insights tailored to the user's local context.

Throughout the framework, green boxes in Figure 1 indicate required inputs (e.g., real-world problem description, observational data, cost parameters), while blue boxes represent the results generated at each step of the process. This integrated framework thus provides a flexible and data-driven approach for guiding intervention decisions during infectious disease outbreaks. The following results are an application of the framework to the early phase of the COVID-19 pandemic in Korea. The objectives are to identify the optimal transmission reduction strategy that minimizes the cost of intervention and infection prior to vaccine development and to provide a dashboard that allows users to control the cost-related parameters.

Mathematical modeling

Figure 2 illustrates the Susceptible(S)-Exposed(E)-Infectious(I)-Isolated(Q)-Recovered(R)-Death(D) (SEIQRD) model to investigate the early phase of COVID-19 in Korea. There are five disease-related parameters (R_0, κ, α, f, and γ): R_0 is the

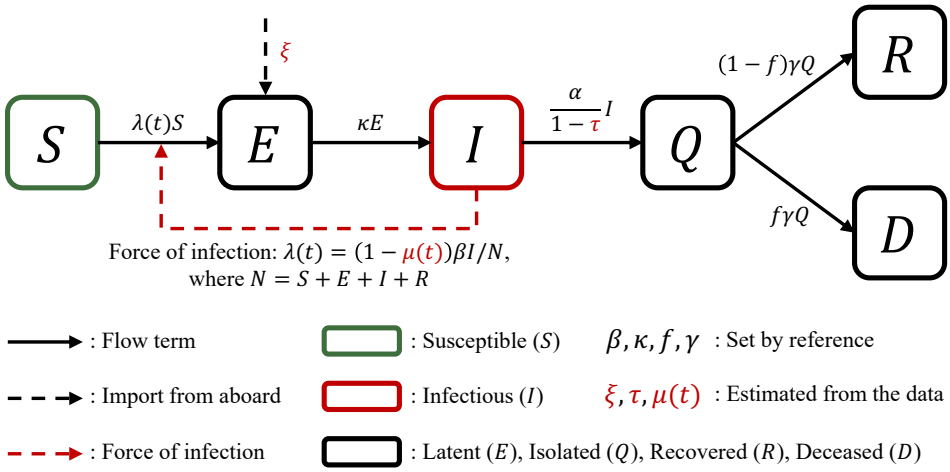

Fig. 2 Mathematical model for infectious diseases. The squares represent compartments of the mathematical model and the black arrows represent flows to the compartments. The black dashed arrow represents external importation which serves as a trigger for an epidemic. The red dashed arrow represents the force of infection which drives the spread of the disease in a country. The parameters in black and red are the disease-related and estimated parameters, respectively.

basic reproductive number of the disease, $1/\kappa$ is the average latent period, $1/\alpha$ is the average infectious period, f is the case fatality rate, and $1/\gamma$ is the average isolation period. There are three policy-related parameters ($\mu(t)$, ξ, and τ): $\mu(t)$ represents the transmission reduction by NPIs, ξ is the average number of imported cases per day, and τ is the average infectious period reduction by NPIs. The details of the mathematical model are presented in the Methods section.

Parameter estimation

Table 1 presents the parameters of the mathematical model. The parameters R_0, $1/\kappa$, $1/\alpha$, and $1/\gamma$ are epidemiological quantities that characterize the disease and whose values can be obtained from a proper reference. However, $\mu(t)$, ξ, and τ may vary across countries or change over time depending on policies or interventions implemented during a given period. Therefore, it is necessary to estimate these unknown parameters and we utilized a hybrid parameter estimation scheme using two global

optimizers to obtain a posterior distribution: the Improved Multi-operator Differential Evolution (IMODE) and the Metropolis-Hastings (MH) algorithm [39], which is one of the Markov Chain Monte Carlo (MCMC) methods [40]. Table 1 shows the estimated values of the policy-related parameters obtained by fitting the model to the cumulative confirmed cases data. The average number of imported cases per day (ξ) is 0.2780, which is approximately 1 person per 4 days. The infectious period reduction (τ) is 62.18%, which means that contact tracing or testing policy reduces the infectious period by that value. The transmission reduction parameter, which has a value between 0 and 0.95, is estimated every two weeks since there were frequent changes in government transmission reduction policies. Note that μ is set to zero during the first two weeks, as confirmed cases were not yet detected. Appendix B presents the correlation between the estimated parameters derived from the MCMC chain.

Table 1 Parameter table for the SEIQRD mathematical model. The symbols, definitions, and values are presented in the table with corresponding references. $\mu(t)$, ξ, and τ are estimated from the cumulative confirmed data.

Symbol	Definition	Value	References
R_0	Basic reproductive number	2.87	[41]
$1/\kappa$	Average latent period	4 (day)	[42]
$1/\alpha$	Average infectious period	10 (day)	[43]
$1/\gamma$	Average isolation period	14 (day)	[44, 45]
f	Case fatality ratio	0.0173	[46]
$\mu(t)$	Transmission reduction by NPIs over time	[0∼0.95]*	estimated
ξ	Average imported cases per day	0.3243* (person/day)	estimated
τ	Average infectious period reduction by NPIs	0.5836*	estimated

*: estimated parameter

Multi-objective optimization

Multi-objective optimization simultaneously minimizes multiple objectives without assigning explicit weights to each one. It identifies Pareto-optimal solutions, where no objective can be improved without compromising at least one of the others. In this work, we employ NSGA-II [47], a multi-objective genetic algorithm, to find Pareto solutions that minimize both infection and intervention costs at the same time. Figure 3(a)

illustrates the objective space, where the average effectiveness of transmission reduction and the number of infections are plotted on the x-axis and y-axis, respectively. Note that each axis represents an objective functional of the multi-objective optimization. Details of the multi-objective optimization are described in the Methods. The black curve indicates the Pareto-optimal solutions obtained from more than a thousand multi-objective optimization results. The colored circles represent Pareto solutions from Strategy 1 (S1) to Strategy 5 (S5), corresponding to scenarios infecting 10% to 0.001% of the population, respectively. The average transmission reduction from S1 to S5 are $32.13\%, 36.60\%, 40.71\%, 47.99\%$, and 58.32%, respectively. The red diamond is estimated strategy (SE) have 53.05% of average transmission reduction and 0.0279% of infected population, which is not on the Pareto curve.

Figure 3(b) shows the corresponding transmission reduction strategies of the selected points in (a). The red curve is the estimated strategy (SE) obtained from the data-fitting process. This curve corresponds to the red diamond in panel (a). Note that every point in the Pareto curve in (a) corresponds to a strategy as in panel (b). Strategies from $S1$ to $S5$ suggest strong intervention policies from 10th week to 2nd week since the detection of index case, respectively. As the average transmission reduction increases, implementing strong policies earlier becomes more favorable. (SE enhanced the transmission reduction from 6th week and it is similar timing with S3. Strategy $S5$ suggests starting a strong policy in the 2nd week after detecting the index case. However, results show that maintaining a prolonged and stringent intervention without breaking is not recommended.

Cost-benefit analysis

Multi-objective optimization yields a set of Pareto-optimal solutions that simultaneously minimize intervention and infection costs, as illustrated in Figure 3(a,b). However, because all Pareto solutions are optimal, no single solution can be deemed

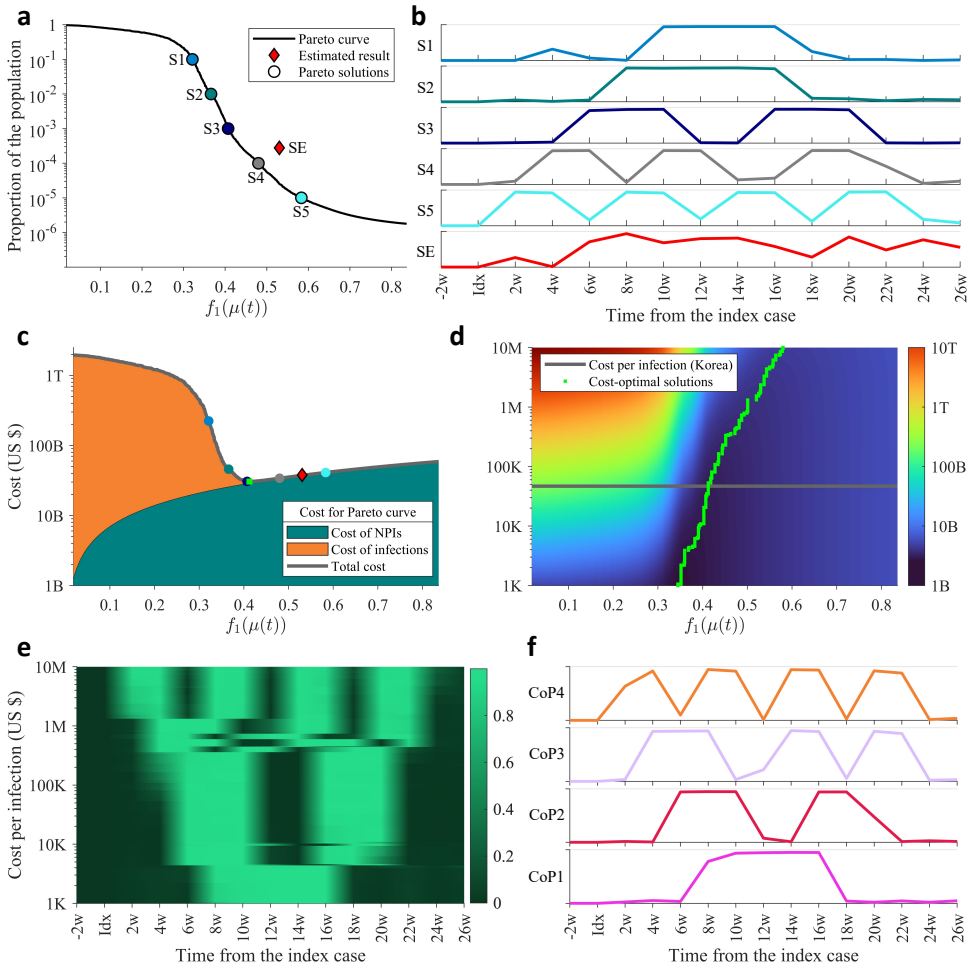

Fig. 3 Cost-benefit analysis results with Pareto solution. (a) Pareto curve and cost-optimal solution. The black solid line, colored circle, and red diamond represent Pareto curve, selected Pareto solution, and estimated point from data, respectively.(b) Corresponding solutions to the points in the panel (a). (c) Total costs of Pareto curve under cost-benefit analysis. Orange area, green area, and gray line represent infection cost, transmission reduction-related intervention cost, and total cost, respectively. (d) Total costs of Pareto curve with different cost per infection. The green points represent cost-optimal solutions with different cost per infection. The gray line corresponds to the panel (c). (e) Cost-optimal solutions for cost per infection. The line parallel to the x-axis represents the cost-optimal solution for the cost per infection and corresponds to the green points in the panel (d). (f) Cost-optimal policy for each cost per infection range.

superior without additional criteria. To address this, we compute the monetary costs of infection and intervention based on simulation results and the country's GDP. The

intervention cost for a strategy is computed as

$$C_{\text{int}}(\mu(t)) = C_1 f_1(\mu(t)) = C_1 \frac{\int_{t_0}^{t_f} \mu(t) dt}{t_f - t_0},$$

where C_1 is the maximum intervention cost in a day, $f_1(\mu(t))$ is the average reduction in relative intervention cost under $\mu(t)$. The infection cost for a strategy is computed as

$$C_{\text{inf}}(\mu(t)) = C_2 f_2(\mu(t)) = C_2 \int_{t_0}^{t_f} \mu(t) \mathcal{R}_0 \frac{\alpha}{1-\tau} I(t) \frac{S(t)}{N(t)} dt,$$

where C_2 is the cost per infection and $f_2(\mu(t))$ is the total infection from t_0 to t_f under $\mu(t)$. The total cost denotes the sum of the intervention cost and infection cost $C_{\text{tot}} = C_{\text{int}} + C_{\text{inf}}$. Details of the cost-benefit analysis are described in the Methods section.

Since a single Pareto point corresponds to a single $f_1(\mu(t))$ value, the x-axis of Figure 3(c,d) corresponds to a Pareto solution. Figure 3(c) shows the cost-benefit analysis results where the cost per infection is set as 39213 USD and the maximum GDP reduction as 4.261%. The orange area represents the cost of infection, the green area represents the cost of transmission reduction intervention, and the gray curve represents the total cost of each strategy. The colored circles are Scenarios S1 to S5, and the red diamond is SE. The green square is the cost-optimal solution for the given cost per infection and intervention cost with an average transmission reduction value of 41.25% and total cost of 30.6B USD. The total costs for strategies S1 to S5, and SE are 223.6B, 45.8B, 30.7B, 34.0B, 41.1B, and 37.9B USD, respectively. The difference between the cost-optimal solution and SE is 7.3B USD and 11.79% in average transmission reduction. Note that if the government implements a weaker strategy than the cost-optimal solution, the total cost increases very rapidly.

Figure 3(d) presents the cost-optimal solution when the cost per infection is changed within the range [1K USD, 10M USD]. For example, if the government implements $f_1(\mu(t)) = 0.3$ strategy and the cost per infection is 10K USD, the expected total cost is 124B USD, according to the heatmap. For each cost per infection, we emphasize the cost-optimal solution as green squares. The gray line is when the cost per infection is 39213 USD, which corresponds to Figure 3(c). If the cost per infection is 1K USD and 10M USD, the total cost of the cost-optimal solution is 25.6B USD and 46.1B USD, respectively. The differences in total cost and average transmission reduction between these two cases are 20.5B USD and 0.2356, respectively. If $f_1(\mu(t)) = 0.3$, the range of total cost is[32.0B USD, 108T USD]. Otherwise, if $f_1(\mu(t)) = 0.5$, the range of total cost is [35.2B USD, 63.9B USD].

Among thousands of Pareto solutions, less than 100 solutions are cost-optimal solutions. Figure 3(e) represents the corresponding cost-optimal solutions according to cost per infection. This figure is an expansion of the green squares in Figure 3(d). The dark green color indicates a weak transmission reduction policy, while the light green color represents a strong transmission reduction policy. Several points of discontinuity can be observed in the cost-optimal solutions with respect to the cost per infection. The cost-optimal pattern (CoP) ranges from CoP1 to CoP3, which are cost-optimal within the intervals [1K,4.41K), [4.41K,361K), [361K,1.33M),and [1.33M,10M] USD, respectively. We note that the cost-optimal pattern for Korea follows CoP2, given that the cost per infection is 39.2K USD. 46.1192 38.9454 37.2855 28.0372 25.6182

Table 2 presents the CoPs corresponding to different ranges of costs per infection. Solutions within each CoP share similar characteristics in terms of the transmission reduction strategy, specifically, the number of intervention periods, the duration of strong interventions, and the start and end time of interventions. This table may guide decision makers in selecting a cost-optimal strategy based on their evaluation of infection and intervention costs.

Table 2 Cost-optimal pattern (CoP) from the index case for cost per infection.

Cost per infection (USD)	Scenario	Strategy pattern (week)				Total cost (USD)	Total infection
		Begin	Increase	Strong	Decrease		
1.33M –	CoP4	0	0–1, 6–7, 12–13,18–19	2–3,8–9, 14–15,20–21	4–5,10–11, 16–17,22–23	38.96B – 46.12	0.00103% – 0.00338%
361K – 1.33M	CoP3	2	2–3, 10–13, 18–19	4–7, 14–15, 20–21	8–9, 16–17 22–23	38.96B – 37.29B	0.00338% – 0.00678%
4.41K – 361K	CoP2	4	4–5, 14–15	6–9, 16–17	10–11, 18–21	28.04B – 37.29B	0.00678% – 0.467%
– 4.41K	CoP1	6	6-7	8–15	16–17	25.62B – 28.04B	0.467% – 2.62%

User-interactive dashboard

Since intervention and infection costs are not only difficult to estimate but also vary widely across settings and individuals, we developed an interactive dashboard using Python Shiny that allows users to adjust cost-related parameters, including GDP, GDP reduction, value of a statistical life (VSL), and the fatality rate. Figure 4, a snapshot of our dashboard, shows the cost-related parameters that users can adjust accordingly. By default, the dashboard is initialized with characteristics of COVID-19 and estimated parameters derived from data of the Republic of Korea. Beneath the parameter adjustment panel, there are model simulation results based on the demography-related, disease-related, and policy-related parameters.

The results in the right panel are similar to the results in Figure 3. The primary difference between the results displayed in the dashboard and those reported in this paper is that the cost-optimal results can be changed by adjusting the cost-related parameters, the quarantine period, and the fatality rate. When users adjust these parameters, the cost-optimal results are updated immediately: the cost-optimal solution is indicated by a green circle, the cost-optimal strategy is represented by a green line, the cost per infection is depicted by a gray dotted line, and the cost-optimal pattern is marked by a non-blurred line. Finally, our dashboard enables policymakers

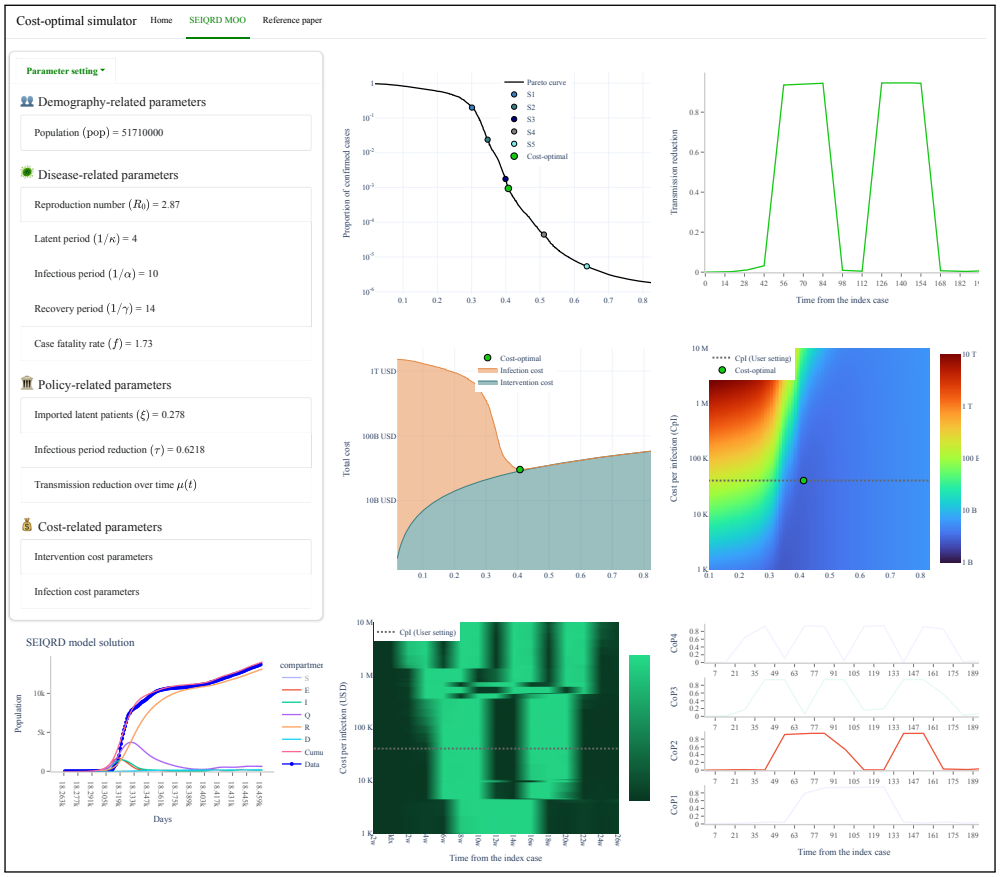

Fig. 4 Interactive dashboard The left panel features a slider bar that allows users to adjust cost-related inputs, while the right panel displays the corresponding simulation results along with a summary of the cost-benefit analysis.

to evaluate the cost-optimal solution based on their perspective immediately and to contextualize their plans by suggesting other possible cost-optimal options.

Discussion

The results presented offer retrospective insights into the COVID-19 pandemic in Korea. However, because the data are only used to estimate unknown parameters of an infectious disease model, the framework can be readily adapted for prospective applications to support scientifically informed decision-making in future infectious disease

outbreaks, particularly in identifying cost-optimal intervention strategies. To apply the framework to an emerging or unknown infectious disease, one needs to make informed assumptions about the disease's epidemiological characteristics, the country-specific responses, and the functional relationship between model outputs and associated economic costs. Based on these assumptions, the framework can simulate the introduction of the disease into a population via importation and identify Pareto-optimal and cost-optimal intervention strategies. To obtain results for different infectious diseases, users can modify the disease-related parameter using values from existing literature [48–50], and then apply our framework. Similarly, to adapt the analysis to different countries, users can adjust the population and policy-related parameters based on the data. Since the policy-related parameters that capture the effects of interventions are estimated using a specific country's data, cost-optimal solutions for other countries can be similarly derived using their country's respective data.

While the research framework makes it possible for policymakers to find a cost-optimal solution under their cost-related parameter setting, the results derived from this framework suggest that the relationship between the transmission reduction and economic cost determines the cost-optimal intervention strategy. If the relationship is linear as we have assumed in the main text, the cost-optimal solutions are on-off type, indicating that the lockdown policy is more cost-effective than other strategies. This supports the intervention strategy implemented in most countries. However, if mask-wearing intervention is cheap and effective, and strong intervention is expensive and ineffective, the early and constant intervention is more effective than other strategies. This means that wearing masks and personal hygiene policies are more cost-effective than the lockdown policy. Therefore, research on intervention cost is crucial as it significantly influences the cost-optimal strategy to implement during an epidemic.

In this research, we only considered controlling transmission-related interventions to obtain a Pareto optimal solution. However, optimal strategies on quarantine and testing are also important to assess during a pandemic [44, 45].

Although our proposed framework provides a way to analyze cost-free and cost-optimal intervention strategies, there are limitations to its practical implementation. First, we adopted the established SEIQR model, which allows for rapid experimentation and generation of results. While the framework emphasizes structural design, it remains flexible. Users can readily incorporate more complex models [51], without the need for algebraic derivations, due to the implementation of the metaheuristic algorithm [39, 47]. Second, if users wish to change the model, the objective functions, or certain parameters, they can obtain different Pareto solutions. Appendix **??** suggests that we can observe a similar cost-optimal pattern under different simulation settings. Additionally, as long as users calculate the Pareto solutions, they can only change the cost-related parameters to obtain a user-defined cost-optimal solution. Third, the theoretical solution does not provide specific policies to achieve the suggested transmission reduction value. Policymakers should refer to other papers on the relationship between transmission reduction and specific policies [52–54]. Lastly, we considered only the cost of infection without accounting for medical resources or potential overburdening, and detailed costs of other interventions such as limitations in gathering, quarantine, testing, and other interventions. Nevertheless, the user can modify the cost of intervention or infection to account for additional intervention or infection costs by adjusting these costs to obtain corresponding cost-optimal solutions.

We formulate the mathematical model considering the importation of infected people from abroad, transmission reduction, and infectious period reduction, which are related to intervention policies during the early phase of a pandemic. Since the effect of interventions is not known, these parameters are estimated using the parameter estimation method, utilizing the hybrid method of a machine learning-based global

optimization (IMODE) and the statistical optimization method (MCMC). Using the mathematical model with estimated parameters, multi-objective optimization obtains Pareto solutions of the transmission reduction policy that simultaneously minimizes the cost of intervention and the cost of infection. Thereafter, cost-benefit analysis determines the cost-optimal solution among the Pareto solutions for a cost per infection; e.g., the higher the cost per infection, the stronger the cost-optimal intervention. Since the cost-optimal solution is changed by the cost of interventions or infection, we build a web-based dashboard that enables customizing the cost and obtaining the corresponding cost-optimal strategy. This research framework can be applied to other respiratory infectious diseases at the beginning of a pandemic.

Methods

Mathematical Modeling

To describe the transmission dynamics of the early phase of the COVID-19 pandemic in Korea, we propose an extended SEIQRD compartmental model. The population is divided into six epidemiological compartments: Susceptible individuals (S) have no immunity and have not yet been exposed to the disease. Latent or exposed individuals (E) have been exposed to the disease but are not yet infectious. Infectious individuals (I) have become infectious and can transmit the disease to susceptible individuals. Isolated individuals (Q) have been identified and isolated due to self-reporting or contact tracing. Recovered individuals (R) have recovered from the disease and are assumed to be immune. Deceased individuals (D) have died from the disease.

The governing equations (1–6) represent the changes in each compartment.

$$\frac{dS}{dt} = -\lambda(t)S, \tag{1}$$

$$\frac{dE}{dt} = \lambda(t)S - \kappa E + \xi, \tag{2}$$

$$\frac{dI}{dt} = \kappa E - \frac{\alpha}{1-\tau} I, \tag{3}$$

$$\frac{dQ}{dt} = \frac{\alpha}{1-\tau} I - \gamma Q, \tag{4}$$

$$\frac{dR}{dt} = (1-f)\gamma Q, \tag{5}$$

$$\frac{dD}{dt} = f\gamma Q, \tag{6}$$

where $\lambda(t) = (1-\mu(t))\mathcal{R}_0 \frac{\alpha}{1-\tau} I/N$ is the force of infection, $\mathcal{R}_0$ is the basic reproduction number, $1/\alpha$ is the average infectious period, τ is the infectious period reduction due to testing or contact tracing policies, $\mu(t)$ is the time-dependent transmission reduction resulting from policy interventions, and $N = S+E+I+R$. The parameter $\mu(t)$ consists of a set of values μ_i, each representing the level of transmission reduction during a specific period. The index i corresponds to the period starting on day $14 \times (i-1)$ from the beginning of the simulation, with each period spanning two weeks. The details on $\mu(t)$ are described in Appendix A. The paremeter ξ is the average daily imported cases to the country; $1/\kappa$ is the mean latent period, that is, the average time to be infectious from the infection; $1/\gamma$ is the average removal period, that is, the average time to recover or die from the disease since isolation; and f is the fatality rate, that is, the probability of death among infected cases. Note that the infectious period does not begin with the onset of symptoms, but rather with the start of infectiousness. For example, patients infected by COVID-19 can be infectious two days before symptoms appear [55]. Figure 2 represents the flowchart of the model.

Data-fitting Process

We utilize two global optimizers—Improved Multi-operator Differential Evolution (IMODE) and Markov Chain Monte Carlo (MCMC)—to estimate the parameters [39, 40, 56]. IMODE achieved first place in the Congress on Evolutionary Computation (CEC) 2020 competition on bounded single-objective optimization algorithms.

It combines the advantages of global and local search, focusing on exploration at the beginning and exploitation at the end of the optimization process. IMODE excels at finding optimal solutions for given function evaluations within a specified domain without a preset initial point. We employ IMODE to minimize the difference between model simulation results and the cumulative confirmed cases data (C_{data}).

$$\min_{\theta} \int_{t_0}^{t_{end}} \left\| \frac{\alpha}{1-\tau} I(t;\theta) - C_{data} \right\|_2 dt \tag{7}$$

where $\theta \in \{\xi, \tau, \mu(t)\}$ are the policy-related parameters.

Sensitivity analysis

The sensitivity analysis results show the relative impact of each parameter on the model outputs. It can provide information on which parameter may effectively control the outputs or which parameter can be ignored. We performed Partial Rank Coefficient Correlation (PRCC) analysis on the number of infected cases and confirmed cases to assess the sensitivity of the paremeters to these model outputs. Note that the confirmed cases are an output for the parameter estimation and the infected cases are an output for the multi-objective optimization. μ and τ are the most sensitive parameters for both outputs among the policy-related parameters, where those parameters affect disease-related parameters β and α. The PRCC results are presented in the Appendix C.

Multi-objective optimization

We assume that interventions affecting the infectious period and the number of imported cases during an epidemic remain fixed, as these are largely determined by a country's health or medical system. In the multi-objective optimization, we focus solely on changes in the transmission reduction parameter $\mu(t)$, which is influenced by government policies such as mask-wearing, social distancing, and gathering restrictions. The goals of the optimization are to simultaneously minimize both infection

levels and the costs associated with transmission-related interventions by adjusting $\mu(t)$. Since $\mu(t)$ represents time-dependent transmission reduction and the expression $\int_{t_0}^{t_f} \mu(t)\mathcal{R}_0\alpha(1-\tau)I(t)\frac{S(t)}{N(t)}dt$ reflects the total number of infections over the simulation period, the two objectives correspond to intervention stringency and epidemic size, respectively. However, directly quantifying the relationship between $\mu(t)$ and the cost of the intervention is difficult. To address this, we assume that the cost of intervention is proportional to both its effectiveness and stringency. Similarly, the cost of infection is assumed to be proportional to the total number of infections. Hence, we minimize the functions $f_1(\mu(t))$ and $f_2(\mu(t))$ represented by

$$\underset{\mu(t)}{\arg\min} \begin{bmatrix} f_1\left(\mu\left(t\right)\right) \\ f_2(\mu(t)) \end{bmatrix} = \underset{\mu(t)}{\arg\min} \begin{bmatrix} \frac{\int_{t_0}^{t_f} \mu(t)dt}{t_f - t_0} \\ \int_{t_0}^{t_f} \mu(t)\mathcal{R}_0\alpha I(t)\frac{S(t)}{N(t)}dt \end{bmatrix}. \tag{8}$$

Note that f_1 and f_2 are proportional to the monetary cost but do not exactly equal the cost. The multi-objective optimization problem simultaneously minimizes f_1 and f_2 where the governing equations are given by equation ((1)–(6)).

The multi-objective optimization will find solutions near the Pareto curve, that is, a set of Pareto solutions in the objective plane composed of the codomain of f_1 and f_2. A solution is considered Pareto-optimal if it is not dominated by any other solution; that is, no other solution performs better in at least one objective without performing worse in at least one other objective. We obtained the Pareto curve using the built-in function *multiobjga* that employs the non-dominated sorting genetic algorithm II (NSGA-II) in MATLAB [47]. To get an accurate solution, we independently run *multiobjga* one thousand times and assembled the Pareto solution by finding the Pareto front.

Cost-Benefit Analysis

Since the Pareto solutions are outputs and not costs, we introduce C_1 as the maximum intervention cost in a day and C_2 as the cost per infection, to convert the outputs into

monetary costs. We consider C_1 to be proportional to two factors: the GDP per capita of the country and the reduction of the GDP by intervention. The GDP of the Republic of Korea in 2019 is 31902, and the maximum reduction is assumed to be 4.26% based on the difference between the GDP projection by OECD in 2019 and the real GDP data [57, 58]. C_2 is divided into the average hospitalization cost and expected cost of death [34–36, 59, 60]. The following are the formulas used for C_1 and C_2:

$$C_1 = \text{GDP} \times \text{GDP}_{\text{MaxRed}} \tag{9}$$

$$C_2 = C_{\text{H}} + f \times \text{VSL}, \tag{10}$$

where GDP is total GDP of the country, $\text{GDP}_{\text{MaxRed}}$ is the maximum GDP reduction by transmission reduction intervention, C_{H} is the average hospitalization cost per infection, f is case fatality rate, and VSL is the value of statistical life. Details of the cost-benefit analysis are described in the Appendix.

Dashboard

The parameters in equations C_1 and C_2 are difficult to specify as single fixed values. For example, VSL can change according to average age, wage, income elasticities, and ethical considerations [61–65]. To address this variability, we developed a dashboard that enables users to select their own cost-related parameters and obtain cost-optimal results within seconds. We built the web dashboard using the Shiny package in Python and included both a mathematical model simulator and a cost-optimal intervention policy simulator. In the mathematical model simulator, users can change various parameters of the SEIQRD model and check the simulation results immediately. In the cost-optimal intervention policy simulator, users can adjust the five economic-related

parameters, which are inputs to the costs C_1 and C_2. This real-time optimization simulator is possible because the multi-objective optimization does not require a weight parameter for each objective.

Supplementary information.

Declarations

Funding

This research is supported by the Bio&Medical Technology Development Program of the National Research Foundation (NRF) funded by the Korean government (MSIT) (RS-2023-00227944). This paper is supported by the Korea National Research Foundation (NRF) grant funded by the Korean government (MEST) (NRF-2021R1A2C100448711).

Data and material availability

All the data, confirmed cases, death cases are uploaded in the Gibhub. The dashboard can be accessible via https://jongmin-lee.shinyapps.io/demomookorea/.

Code availability

The results can be generated by the attached code in Github https://github.com/ljm1729-scholar/MOO_framework.

Author contribution

- Funding
- Conflict of interest/Competing interests (check journal-specific guidelines for which heading to use)
- Ethics approval and consent to participate

- Consent for publication

If any of the sections are not relevant to your manuscript, please include the heading and write 'Not applicable' for that section.

Appendix A Transmission reduction $\mu(t)$

The time-dependent transmission reduction function $\mu(t)$ is defined using linear interpolation of μ_i, that is, the transmission reduction at time $t = i \times 14$:

$$\mu(t) = \mu_{n+1} - \left(n - \frac{t}{14}\right)(\mu_{n+1} - \mu_n), \tag{A1}$$

where $n = \lceil \frac{t}{14} \rceil$ and $\mu_0 = 0$. Note that we assume transmission reduction changes every two weeks, in accordance with government announcements regarding adjustments in intervention strategies. We also assume that testing and controlling of imported cases are implemented by the government. The parameter ξ represents the mean daily imported cases per day. The imported cases are affected by the screening system in the airports or borders. We assume that there are no infected cases at the beginning of the simulation since the spread of infectious diseases are triggered by imported cases. The parameter τ represents the infectious period reduction that is affected by the testing or tracing system of the government. We estimated these policy-related parameters from the confirmed cases data.

Appendix B Hybrid parameter estimation

To reduce computational time and find a more accurate solution, we utilized two algorithms – the global optimization algorithm named improved multi-operator differential evolution (IMODE) and the Markov-chain Monte Carlo (MCMC) method. In our simulations, we used the cumulative confirmed cases data and minimized the $L2$-norm between the data and the corresponding output from the simulation results. We estimated the policy-related parameters ξ, τ, μ_3, μ_4, $\cdots$ as described in the main text. IMODE finds the optimal solution faster and the MCMC provides the solution with posterior information.

B.1 Improved multi-operator differential evolution

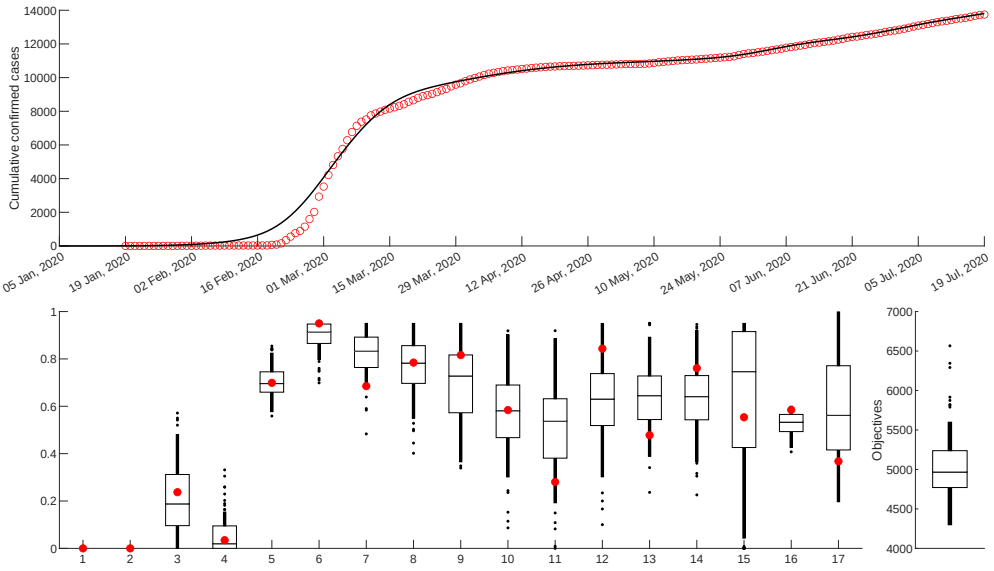

Fig. B1 IMODE estimation results. (A) shows the cumulative confirmed cases and simulation results. (B) shows the 25 estimation results with boxchart and the best estimation results with red circle point. (C) shows the L2-norm of 25 estimation results.

If a local optimizer is used, user-specified initial values must often be taken into account, since the solution may be sensitive to the starting point. The use of a global optimizer eliminates this problem since it does not require an initial value for the optimization. To reduce the randomness of the global optimizer, we run IMODE twenty-five times and select the best solution among them [39]. Each simulation terminates after 100,000 function evaluations. Figure B1 shows the estimation results. Since the IMODE algorithm can search for the most suitable solution in the loss landscape, we used the IMODE results as prior information in the MCMC process.

B.2 MCMC process

We use the MATLAB package to run the Markov-chain Monte-Carlo (MCMC) algorithm [40, 56]. This package requires the parameter list, prior distribution of the

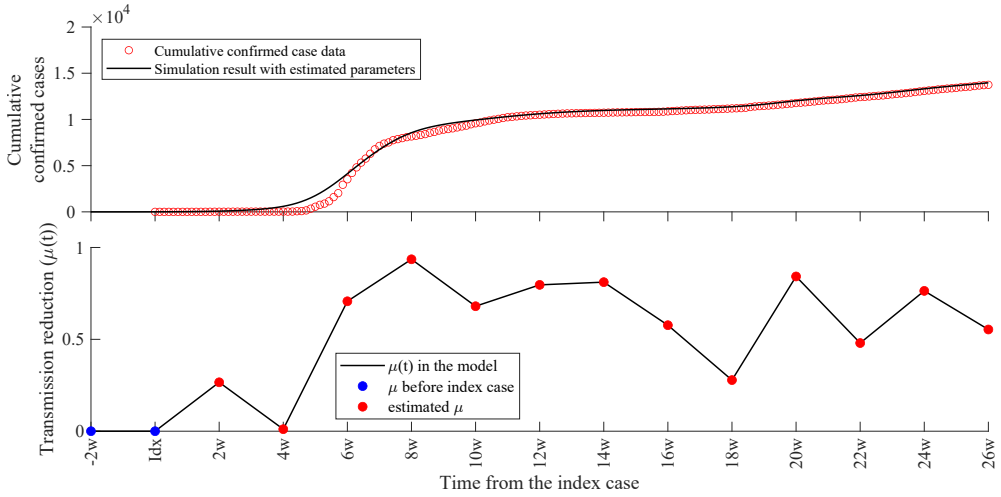

Fig. B2 MCMC estimation results. (A) shows the cumulative confirmed cases and simulation results. (B) show the estimated $\mu(t)$. (C) shows the daily confirmed cases and simulation results.

parameters, the equations of the system, and the objective function of the MCMC process. The package uses the delayed-rejection adaptive metropolis (DRAM) algorithm [56] to search for the posterior distribution. We set the prior distribution as a normal distribution that has a mean value from the IMODE results and a standard deviation of 0.05. Figure B2 shows the parameter estimation results.

Figure B3 presents the MCMC chains obtained from the DRAM algorithm. The total length of the chain is 1 million, where the burn-in period is half of the total chain length. The red lines indicate the burn-in period, and the rest of the chain composes the posterior distribution.

Figure B4 presents the correlation between the estimated parameters derived from the MCMC chain. Many of the elements have correlation values lower than 0.5 except for the diagonal part. The lower correlation values indicate the practical identifiability of the estimated parameters.

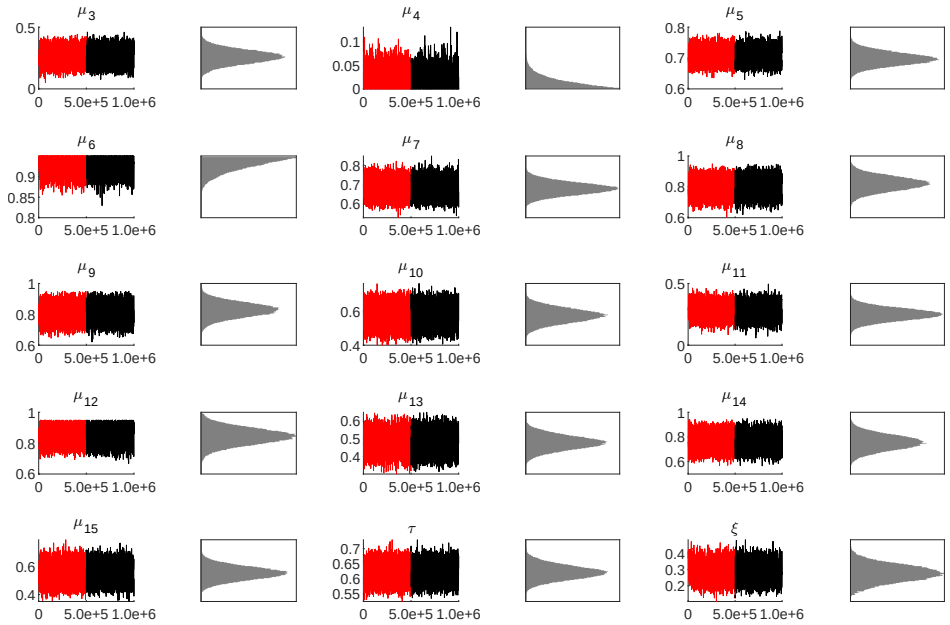

Fig. B3 MCMC chain for the estimated parameters. The red period indicate the burn-in that is half of the total iteration. The black period composes the posterior distribution

Appendix C Sensitivity analysis results

Sensitivity analysis presents how impactful the parameters are on the simulation results. We set μ as constant in this sensitivity analysis simulation. We check the sensitivity for two outputs – cumulative confirmed cases and the number of infections. The cumulative cases are used for the data-fitting process and the number of infections is used for the multi-objective optimization. Figure C5 presents the PRCC results for two outputs. The β has the highest correlation and is larger than 0.8 for all time. κ and ξ have 0.6723 and 0.6203 at the beginning of the simulation but they monotonically reduce to 0.2432 and 0.0837, respectively. τ is 0.5 at the beginning of the simulation but the correlation keeps increasing up to 0.8.

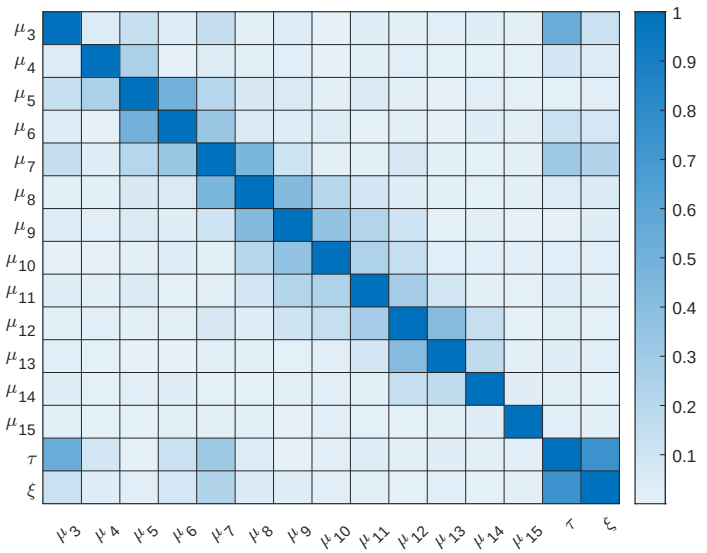

Fig. B4 Correlation between the estimated parameters. The white color indicate the lower correlation and blue color indicate the higher correlation.

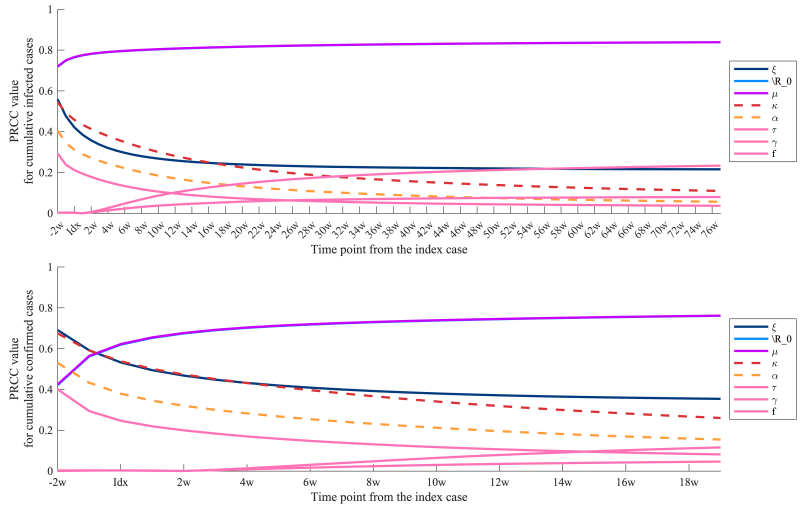

Fig. C5 Parameter estimation results. Correlation between the model simulation and parameter over time. Solid and dashed line indicate positive and negative correlation, respectively.

References

[1] Pangallo, M. *et al.* The unequal effects of the health–economy trade-off during the covid-19 pandemic. *Nature Human Behaviour* **8**, 264–275 (2024). URL https:

//doi.org/10.1038/s41562-023-01747-x.

[2] Carrieri, V., De Paola, M. & Gioia, F. The health-economy trade-off during the covid-19 pandemic: Communication matters. *PLOS ONE* **16**, 1–25 (2021). URL https://doi.org/10.1371/journal.pone.0256103.

[3] Whitehead, S. J. & Ali, S. Health outcomes in economic evaluation: the qaly and utilities. *British Medical Bulletin* **96**, 5–21 (2010). URL https://doi.org/10.1093/bmb/ldq033.

[4] O'Mahony, J. F., Newall, A. T. & van Rosmalen, J. Dealing with time in health economic evaluation: Methodological issues and recommendations for practice. *PharmacoEconomics* **33**, 1255–1268 (2015). URL https://doi.org/10.1007/s40273-015-0309-4.

[5] Stamuli, E. Health outcomes in economic evaluation: who should value health? *British Medical Bulletin* **97**, 197–210 (2011). URL https://doi.org/10.1093/bmb/ldr001.

[6] Findlater, A. & Bogoch, I. I. Human mobility and the global spread of infectious diseases: A focus on air travel. *Trends in Parasitology* **34**, 772–783 (2018). URL https://doi.org/10.1016/j.pt.2018.07.004.

[7] Baker, R. E. *et al.* Infectious disease in an era of global change. *Nature Reviews Microbiology* **20**, 193–205 (2022). URL https://doi.org/10.1038/s41579-021-00639-z.

[8] Wilder-Smith, A. & Freedman, D. O. Isolation, quarantine, social distancing and community containment: pivotal role for old-style public health measures in the novel coronavirus (2019-ncov) outbreak. *Journal of Travel Medicine* **27**, taaa020 (2020). URL https://doi.org/10.1093/jtm/taaa020.

[9] Sachs, J. D. *et al.* The lancet commission on lessons for the future from the covid-19 pandemic. *The Lancet* **400**, 1224–1280 (2022). URL https://doi.org/10.1016/S0140-6736(22)01585-9.

[10] Michie, S. & West, R. Behavioural, environmental, social, and systems interventions against covid-19. *BMJ* **370** (2020). URL https://www.bmj.com/content/370/bmj.m2982.

[11] Gumel, A. B., Iboi, E. A., Ngonghala, C. N. & Elbasha, E. H. A primer on using mathematics to understand covid-19 dynamics: Modeling, analysis and simulations. *Infectious Disease Modelling* **6**, 148 – 168 (2021). URL https://www.scopus.com/inward/record.uri?eid=2-s2.0-85098540975&doi=10.1016%2fj.idm.2020.11.005&partnerID=40&md5=749b44a947056cf2279e309b70f236a9. Cited by: 140; All Open Access, Gold Open Access, Green Open Access.

[12] Abueg, M. *et al.* Modeling the effect of exposure notification and non-pharmaceutical interventions on covid-19 transmission in washington state. *npj Digital Medicine* **4** (2021). URL https://www.scopus.com/inward/record.uri?eid=2-s2.0-85102502833&doi=10.1038%2fs41746-021-00422-7&partnerID=40&md5=48f8debe9fa5f346aebdc522eb57364e. Cited by: 60; All Open Access, Gold Open Access, Green Open Access.

[13] Davies, N. G. *et al.* Effects of non-pharmaceutical interventions on covid-19 cases, deaths, and demand for hospital services in the uk: a modelling study. *The Lancet Public Health* **5**, e375 – e385 (2020). URL https://www.scopus.com/inward/record.uri?eid=2-s2.0-85086675142&doi=10.1016%2fS2468-2667%2820%2930133-X&partnerID=40&md5=50e600bca0db8f62284699374f122f50. Cited by: 584; All Open Access, Gold Open Access, Green Open Access.

[14] Hao, X. *et al.* Reconstruction of the full transmission dynamics of covid-19 in wuhan. *Nature* **584**, 420 – 424 (2020). URL https://www.scopus.com/inward/record.uri?eid=2-s2.0-85087949741&doi=10.1038%2fs41586-020-2554-8&partnerID=40&md5=691aa394cc4fe2cfdf7d83336fe6f6bb. Cited by: 338; All Open Access, Hybrid Gold Open Access.

[15] López, L. & Rodó, X. The end of social confinement and covid-19 re-emergence risk. *Nature Human Behaviour* **4**, 746 – 755 (2020). URL https://www.scopus.com/inward/record.uri?eid=2-s2.0-85086741830&doi=10.1038%2fs41562-020-0908-8&partnerID=40&md5=75b31d78e0cf6a0aec0a58cda1e6279c. Cited by: 168; All Open Access, Green Open Access, Hybrid Gold Open Access.

[16] Silva, P. C. *et al.* Covid-abs: An agent-based model of covid-19 epidemic to simulate health and economic effects of social distancing interventions. *Chaos, Solitons and Fractals* **139** (2020). URL https://www.scopus.com/inward/record.uri?eid=2-s2.0-85087587605&doi=10.1016%2fj.chaos.2020.110088&partnerID=40&md5=8805893c3f5910fbddf680da19d16b78. Cited by: 337; All Open Access, Green Open Access.

[17] Merler, S. *et al.* Spatiotemporal spread of the 2014 outbreak of ebola virus disease in liberia and the effectiveness of non-pharmaceutical interventions: A computational modelling analysis. *The Lancet Infectious Diseases* **15**, 204 – 211 (2015). URL https://www.scopus.com/inward/record.uri?eid=2-s2.0-84921319630&doi=10.1016%2fS1473-3099%2814%2971074-6&partnerID=40&md5=8ee23784230fab79f81691803cb73f7e. Cited by: 216; All Open Access, Green Open Access.

[18] Hinch, R. *et al.* Openabm-covid19-an agent-based model for non-pharmaceutical interventions against covid-19 including contact tracing. *PLoS Computational*

582 *Biology* **17** (2021). URL https://www.scopus.com/inward/record.uri?eid=2-s2.
583 0-85110953504&doi=10.1371%2fjournal.pcbi.1009146&partnerID=40&md5=
584 069c0897e0a7232bc22d981119ae2aa4. Cited by: 140; All Open Access, Gold
585 Open Access, Green Open Access.

586 [19] Patel, M. D. *et al.* Association of simulated covid-19 vaccination and nonphar-
587 maceutical interventions with infections, hospitalizations, and mortality. *JAMA*
588 *Network Open* **4**, E2110782 (2021). URL https://www.scopus.com/inward/
589 record.uri?eid=2-s2.0-85106982002&doi=10.1001%2fjamanetworkopen.2021.
590 10782&partnerID=40&md5=3022eed51b7c7e725e47514ad0f5bef3. Cited by: 79;
591 All Open Access, Gold Open Access, Green Open Access.

592 [20] Lai, S. *et al.* Effect of non-pharmaceutical interventions to con-
593 tain covid-19 in china. *Nature* **585**, 410 – 413 (2020). URL https:
594 //www.scopus.com/inward/record.uri?eid=2-s2.0-85085062703&doi=10.1038%
595 2fs41586-020-2293-x&partnerID=40&md5=636205284df81a2e02f8bfe142cf2c7b.
596 Cited by: 910; All Open Access, Green Open Access, Hybrid Gold Open Access.

597 [21] Salathé, M. & Jones, J. H. Dynamics and control of diseases in
598 networks with community structure. *PLoS Computational Biology*
599 **6** (2010). URL https://www.scopus.com/inward/record.uri?eid=2-s2.
600 0-77954594423&doi=10.1371%2fjournal.pcbi.1000736&partnerID=40&md5=
601 0db9ae76312c0a744a824e92d1755690. Cited by: 452; All Open Access, Gold
602 Open Access, Green Open Access.

603 [22] Nielsen, B. F., Simonsen, L. & Sneppen, K. Covid-19 superspreading sug-
604 gests mitigation by social network modulation. *Physical Review Letters*
605 **126** (2021). URL https://www.scopus.com/inward/record.uri?eid=2-s2.
606 0-85103315355&doi=10.1103%2fPhysRevLett.126.118301&partnerID=40&

md5=600cdd0cc00630ab644a1dd3d0cc4172. Cited by: 66; All Open Access, Green Open Access, Hybrid Gold Open Access.

[23] Lee, J., Mendoza, R., Mendoza, V. M. P. & Jung, E. Differential evolution with spherical search algorithm for nonlinear engineering and infectious disease optimization problems. *Applied Soft Computing* **168**, 112446 (2025). URL https://www.sciencedirect.com/science/article/pii/S1568494624012201.

[24] Asamoah, J. K. K. *et al.* Global stability and cost-effectiveness analysis of covid-19 considering the impact of the environment: using data from ghana. *Chaos, Solitons and Fractals* **140** (2020). URL https://www.scopus.com/inward/record.uri?eid=2-s2.0-85089263548&doi=10.1016%2fj.chaos.2020.110103&partnerID=40&md5=37ee6e6103ad44333225bdc71215af28. Cited by: 189; All Open Access, Green Open Access.

[25] D'Onofrio, A., Iannelli, M., Manfredi, P. & Marinoschi, G. Optimal epidemic control by social distancing and vaccination of an infection structured by time since infection: The covid-19 case study*. *SIAM Journal on Applied Mathematics* **84**, S199 – S224 (2024). URL https://www.scopus.com/inward/record.uri?eid=2-s2.0-85168717254&doi=10.1137%2f22M1499406&partnerID=40&md5=344dc164a555d07dd4f2ea5f9b76ab24. Cited by: 13; All Open Access, Green Open Access.

[26] Ullah, S. & Khan, M. A. Modeling the impact of non-pharmaceutical interventions on the dynamics of novel coronavirus with optimal control analysis with a case study. *Chaos, Solitons and Fractals* **139** (2020). URL https://www.scopus.com/inward/record.uri?eid=2-s2.0-85087626042&doi=10.1016%2fj.chaos.2020.110075&partnerID=40&md5=ce56cafd4b8ec986a13c9c90adb8ba69. Cited by: 189; All Open Access, Green Open Access.

[27] Perkins, T. A. & España, G. Optimal control of the covid-19 pandemic with non-pharmaceutical interventions. *Bulletin of Mathematical Biology* **82** (2020). URL https://www.scopus.com/inward/record.uri?eid=2-s2.0-85090276965&doi=10.1007%2fs11538-020-00795-y&partnerID=40&md5=70dd7232fff5b1fe1991950ce3a48c3d. Cited by: 114; All Open Access, Green Open Access, Hybrid Gold Open Access.

[28] Balcells, C. C., Krueger, R. & Bierlaire, M. Multi-objective optimization of activity-travel policies for epidemic control: Balancing health and economic outcomes on socio-economic segments. *Transportation Research Interdisciplinary Perspectives* **27** (2024). URL https://www.scopus.com/inward/record.uri?eid=2-s2.0-85200988336&doi=10.1016%2fj.trip.2024.101183&partnerID=40&md5=66efe6d81a05c3a88a7865a40a505a22. Cited by: 1; All Open Access, Gold Open Access.

[29] Tu, Y., Meng, X., Alzahrani, A. K. & Zhang, T. Multi-objective optimization and nonlinear dynamics for sub-healthy covid-19 epidemic model subject to self-diffusion and cross-diffusion. *Chaos, Solitons and Fractals* **175** (2023). URL https://www.scopus.com/inward/record.uri?eid=2-s2.0-85168016075&doi=10.1016%2fj.chaos.2023.113920&partnerID=40&md5=b14cb6424fa2a9d2b09cfc6462b8d8d0. Cited by: 1.

[30] Siebert, B. A., Gleeson, J. P. & Asllani, M. Nonlinear random walks optimize the trade-off between cost and prevention in epidemics lockdown measures: The esir model. *Chaos, Solitons and Fractals* **161** (2022). URL https://www.scopus.com/inward/record.uri?eid=2-s2.0-85132771446&doi=10.1016%2fj.chaos.2022.112322&partnerID=40&md5=afa11a829ddb1236c894f486a15ff560. Cited by: 3; All Open Access, Green Open Access, Hybrid Gold Open Access.

[31] Zhou, X., Zhang, X., Santi, P. & Ratti, C. Phase-wise evaluation and optimization of non-pharmaceutical interventions to contain the covid-19 pandemic in the u.s. *Frontiers in Public Health* **Volume 11 - 2023** (2023). URL https://www.frontiersin.org/journals/public-health/articles/10.3389/fpubh.2023.1198973.

[32] Mendoza, V. M. P., Mendoza, R., Lee, J. & Jung, E. Adjusting non-pharmaceutical interventions based on hospital bed capacity using a multi-operator differential evolution. *AIMS Mathematics* **7**, 19922–19953 (2022). URL https://www.aimspress.com/article/doi/10.3934/math.20221091.

[33] Paltiel, A. D., Zheng, A. & Walensky, R. P. Assessment of sars-cov-2 screening strategies to permit the safe reopening of college campuses in the united states. *JAMA Network Open* **3** (2020). URL https://www.scopus.com/inward/record.uri?eid=2-s2.0-85089116155&doi=10.1001%2fjamanetworkopen.2020.16818&partnerID=40&md5=02a4ce16fed648195f28f87e1aabc64f. Cited by: 314; All Open Access, Gold Open Access, Green Open Access.

[34] Paltiel, A. D., Zheng, A. & Sax, P. E. Clinical and economic effects of widespread rapid testing to decrease sars-cov-2 transmission. *Annals of Internal Medicine* **174**, 803 – 810 (2021). URL https://www.scopus.com/inward/record.uri?eid=2-s2.0-85108303432&doi=10.7326%2fM21-0510&partnerID=40&md5=27e560b6ed11e3c0ea21c91d7a4be112. Cited by: 42; All Open Access, Green Open Access.

[35] Sandmann, F. G. *et al.* The potential health and economic value of sars-cov-2 vaccination alongside physical distancing in the uk: a transmission model-based future scenario analysis and economic evaluation. *The Lancet Infectious Diseases* **21**, 962 – 974 (2021). URL https://www.scopus.com/inward/record.uri?eid=2-s2.0-85103958835&doi=10.1016%2fS1473-3099%2821%2900079-7&partnerID=

40&md5=3dc4b370e73130793890ad7b6965e095. Cited by: 117; All Open Access, Green Open Access, Hybrid Gold Open Access.

[36] Kohli, M. A. *et al.* The potential clinical impact and cost-effectiveness of the updated covid-19 mrna fall 2023 vaccines in the united states. *Journal of Medical Economics* **26**, 1532 – 1545 (2023). URL https://www.scopus.com/inward/record.uri?eid=2-s2.0-85178014810&doi=10.1080%2f13696998.2023.2281083&partnerID=40&md5=e54ceb699445624472d7d1b3639011ee. Cited by: 15; All Open Access, Gold Open Access.

[37] Schapermeier, L., Grimme, C. & Kerschke, P. Plotting impossible? surveying visualization methods for continuous multi-objective benchmark problems. *IEEE Transactions on Evolutionary Computation* **26**, 1306 – 1320 (2022). URL https://www.scopus.com/inward/record.uri?eid=2-s2.0-85140708868&doi=10.1109%2fTEVC.2022.3214894&partnerID=40&md5=727b35ebdb3d72d2ac93a298c61686d0. Cited by: 6.

[38] Zhu, Z. Personalized recommendation algorithm based on data mining and multi-objective immune optimization. *Informatica (Slovenia)* **48**, 131 – 144 (2024). URL https://www.scopus.com/inward/record.uri?eid=2-s2.0-85210314686&doi=10.31449%2finf.v48i19.6546&partnerID=40&md5=a3e09406f5852e7158ec78f333360059. Cited by: 1; All Open Access, Gold Open Access.

[39] Sallam, K. M., Elsayed, S. M., Chakrabortty, R. K. & Ryan, M. J. *Improved multi-operator differential evolution algorithm for solving unconstrained problems*, 1–8 (IEEE, 2020).

[40] Haario, H., Saksman, E. & Tamminen, J. An adaptive metropolis algorithm. *Bernoulli* **7** (2001).

[41] Billah, M. A., Miah, M. M. & Khan, M. N. Reproductive number of coronavirus: A systematic review and meta-analysis based on global level evidence. *PLOS ONE* **15**, 1–17 (2020). URL https://doi.org/10.1371/journal.pone.0242128.

[42] Xin, H. *et al.* Estimating the latent period of coronavirus disease 2019 (covid-19). *Clinical Infectious Diseases* **74**, 1678–1681 (2021). URL https://doi.org/10.1093/cid/ciab746.

[43] Chen, D. *et al.* Inferring time-varying generation time, serial interval, and incubation period distributions for covid-19. *Nature Communications* **13**, 7727 (2022). URL https://doi.org/10.1038/s41467-022-35496-8.

[44] Wells, C. R. *et al.* Optimal covid-19 quarantine and testing strategies. *Nature Communications* **12**, 356 (2021). URL https://doi.org/10.1038/s41467-020-20742-8.

[45] Ashcroft, P., Lehtinen, S., Angst, D. C., Low, N. & Bonhoeffer, S. Quantifying the impact of quarantine duration on covid-19 transmission. *eLife* **10**, e63704 (2021). URL https://doi.org/10.7554/eLife.63704.

[46] World Health Organization. Covid-19 confirmed cases and deaths (processed by our world in data) (2025). URL https://ourworldindata.org/coronavirus. Retrieved June 25, 2025. Data provided by WHO; population estimates from various sources (2024). Processed and hosted by Our World in Data.

[47] Deb, K., Pratap, A., Agarwal, S. & Meyarivan, T. A fast and elitist multiobjective genetic algorithm: Nsga-ii. *IEEE Transactions on Evolutionary Computation* **6**, 182–197 (2002).

[48] van den Driessche, P. Reproduction numbers of infectious disease models. *Infectious Disease Modelling* **2**, 288–303 (2017). URL https://www.sciencedirect.com/

science/article/pii/S2468042717300209.

[49] Lessler, J. *et al.* Incubation periods of acute respiratory viral infections: a systematic review. *The Lancet Infectious Diseases* **9**, 291–300 (2009). URL https://www.sciencedirect.com/science/article/pii/S1473309909700696.

[50] Vink, M. A., Bootsma, M. C. J. & Wallinga, J. Serial intervals of respiratory infectious diseases: A systematic review and analysis. *American Journal of Epidemiology* **180**, 865–875 (2014). URL https://doi.org/10.1093/aje/kwu209.

[51] Hong, H. *et al.* Overcoming bias in estimating epidemiological parameters with realistic history-dependent disease spread dynamics. *Nature Communications* **15**, 8734 (2024). URL https://doi.org/10.1038/s41467-024-53095-7.

[52] Flaxman, S. *et al.* Estimating the effects of non-pharmaceutical interventions on covid-19 in europe. *Nature* **584**, 257–261 (2020). URL https://doi.org/10.1038/s41586-020-2405-7.

[53] Haug, N. *et al.* Ranking the effectiveness of worldwide covid-19 government interventions. *Nature Human Behaviour* **4**, 1303–1312 (2020). URL https://doi.org/10.1038/s41562-020-01009-0.

[54] Brauner, J. M. *et al.* Inferring the effectiveness of government interventions against covid-19. *Science* **371**, eabd9338 (2021). URL https://www.science.org/doi/abs/10.1126/science.abd9338.

[55] Tindale, L. C. *et al.* Evidence for transmission of covid-19 prior to symptom onset. *eLife* **9**, e57149 (2020). URL https://doi.org/10.7554/eLife.57149.

[56] Haario, H., Laine, M., Mira, A. & Saksman, E. Dram: Efficient adaptive mcmc. *Statistics and Computing* **16**, 339–354 (2006). URL https://doi.org/10.1007/

s11222-006-9438-0.

[57] World Bank. World Development Indicators: GDP per capita (current US$) (NY.GDP.PCAP.CD). World Bank Group (2024). URL https://data.worldbank.org/indicator/NY.GDP.PCAP.CD. Accessed 22 June 2025, CC BY 4.0.

[58] Organisation for Economic Co-operation and Development. Real GDP forecast (indicator). OECD Data (2025). Accessed 22 June 2025.

[59] Rocha-Filho, C. R. *et al.* Hospitalization costs of coronaviruses diseases in upper-middle-income countries: A systematic review. *PLOS ONE* **17**, 1–13 (2022). URL https://doi.org/10.1371/journal.pone.0265003.

[60] Sweis, N. J. Revisiting the value of a statistical life: an international approach during covid-19. *Risk Management* **24**, 259–272 (2022). URL https://doi.org/10.1057/s41283-022-00094-x.

[61] Kip Viscusi, W. & Aldy, J. E. Labor market estimates of the senior discount for the value of statistical life. *Journal of Environmental Economics and Management* **53**, 377–392 (2007). URL https://www.sciencedirect.com/science/article/pii/S0095069607000034.

[62] Aldy, J. E. & Viscusi, W. K. Age differences in the value of statistical life: Revealed preference evidence. *Review of Environmental Economics and Policy* **1**, 241–260 (2007). URL https://doi.org/10.1093/reep/rem014.

[63] Robinson, L. A., Hammitt, J. K. & O'Keeffe, L. Valuing mortality risk reductions in global benefit-cost analysis. *Journal of Benefit-Cost Analysis* **10**, 15–50 (2019).

[64] Madheswaran, S. Measuring the value of statistical life: estimating compensating wage differentials among workers in india. *Social Indicators Research* **84**, 83–96

(2007). URL https://doi.org/10.1007/s11205-006-9076-0.

[65] Viscusi, W. K. & Aldy, J. E. The value of a statistical life: A critical review of market estimates throughout the world. *Journal of Risk and Uncertainty* **27**, 5–76 (2003). URL https://doi.org/10.1023/A:1025598106257.